

# Ionic Liquids: Dissecting the Enthalpies of Vaporization

Thorsten Köddermann,<sup>[a]</sup> Dietmar Paschek,<sup>\*,[b]</sup> and Ralf Ludwig<sup>\*,[a, c]</sup>

We calculate the heats of vaporisation for imidazolium-based ionic liquids  $[C_n\text{mim}][\text{NTf}_2]$  with  $n = 1, 2, 4, 6, 8$  by means of molecular dynamics (MD) simulations and discuss their behavior with respect to temperature and the alkyl chain length. We use a force field developed recently. The different cohesive energies contributing to the overall heats of vaporisations are discussed in detail. With increasing alkyl chain length, the Coulomb contribution to the heat of vaporisation remains constant at around

$80 \text{ kJ mol}^{-1}$ , whereas the van der Waals interaction increases continuously. The calculated increase of about  $4.7 \text{ kJ mol}^{-1}$  per  $\text{CH}_2$ -group of the van der Waals contribution in the ionic liquid exactly coincides with the increase in the heats of vaporisation for  $n$ -alcohols and  $n$ -alkanes, respectively. The results support the importance of van der Waals interactions even in systems completely composed of ions.

## 1. Introduction

Room-temperature ionic liquids (RTILs) are salts with melting points below  $100^\circ\text{C}$ . These substances are receiving an increasing amount of attention on account of their application as alternative solvents due to their physicochemical properties. Among other interesting features, ILs show extremely low vapor pressures and thus can be substitutes for traditional industrial solvents such as volatile organic compounds. The low volatility and the corresponding high heats of vaporization make them attractive as "green" solvents.<sup>[1–3]</sup>

For a long time the vapor pressures of ionic liquids were considered too low to be measured. Consequently there have been no studies of the nature of the vapor and no direct determination of heats of vaporisation. Meanwhile the first qualitative distillation experiments underlined the very low volatility of ILs<sup>[4,5]</sup> and the first quantitative measurements of the vapor pressures and heats of vaporisation of imidazolium based ILs have been reported.<sup>[6–9]</sup> Estimates for the heats of vaporisation from molecular dynamics (MD) simulations,<sup>[9–12]</sup> and the COSMO-RS method<sup>[13]</sup> were also given. Most of the experiments and calculations were performed with 1-alkyl-3-methylimidazolium bis(trifluoromethylsulfonyl)imide  $[C_n\text{mim}][\text{NTf}_2]$  ( $n = 2–10$ ). This family of ionic liquids is known for its thermal stability.

Although some measured and calculated heats of vaporisation for imidazolium-based ILs  $[C_n\text{mim}][\text{NTf}_2]$  are available today, (see Table 1) the situation is still not satisfying. Depending on the experimental methods, values for the heats of vaporisation for these ILs can differ by up to  $50 \text{ kJ mol}^{-1}$  (Figure 1). This amount of energy easily includes the heat of vaporisation  $\Delta H_{\text{vap}}(298)$  of water ( $43.99 \text{ kJ mol}^{-1}$ ) or low-chain  $n$ -alcohols such as ethanol ( $42.32 \text{ kJ mol}^{-1}$ ). Obviously a sub-

stantial amount of interaction is either missing or overestimated. In particular, the slopes of  $\Delta H_{\text{vap}}(298)$  values for  $[C_n\text{mim}][\text{NTf}_2]$  with  $n = 1–8$  differ by a factor of up to two using several experimental techniques. Some important questions arise: How reliable are the given experiments? What is supposed to be the best method to measure enthalpies of vaporisation? And finally: What is the origin of the absolute  $\Delta H_{\text{vap}}(T)$  values and how does this property depend on temperature and on the alkyl chain length of the imidazolium cation? Herein, we study thermodynamic properties such as heats of vaporisation for imidazolium-based ILs  $[C_n\text{mim}][\text{NTf}_2]$  by using MD simula-

**Table 1.** Molar enthalpies of vaporization,  $\Delta_{\text{vap}}H(298)$  in  $\text{kJ mol}^{-1}$  of ionic liquids  $[C_n\text{MIM}][\text{NTf}_2]$  obtained by various experimental methods compared to results from MD simulations.

Ionic Liquid	Knudsen <sup>[6]</sup>	Surface Tension <sup>[6]</sup>	TPD <sup>[7]</sup>	Transpiration <sup>[8]</sup>	Microcalorimetry <sup>[9]</sup>	MD Simulations <sup>[9]</sup>	MD Simulations <sup>[10]</sup>
$[C_1\text{MIM}][\text{NTf}_2]$							$132.1 \pm 0.3$
$[C_2\text{MIM}][\text{NTf}_2]$	135.3	136.1	134	$136.7 \pm 3.4$	136	$159 \pm 10$	$130.6 \pm 0.4$
$[C_4\text{MIM}][\text{NTf}_2]$	136.2	134.6	134		155	$174 \pm 11$	$135.1 \pm 0.6$
$[C_6\text{MIM}][\text{NTf}_2]$	139.8	141.6	139		173	$184 \pm 7$	$143.8 \pm 0.6$
$[C_8\text{MIM}][\text{NTf}_2]$	150.0	149.0	149		192	$201 \pm 6$	$153.6 \pm 0.9$

[a] T. Köddermann, Prof. Dr. R. Ludwig  
Institut für Chemie, Abteilung Physikalische Chemie  
Universität Rostock  
Dr.-Lorenz-Weg 1, 18059 Rostock (Germany)  
Fax: (+49) 381-498-6524  
E-mail: ralf.ludwig@uni-rostock.de

[b] Dr. D. Paschek  
Fakultät Chemie, Physikalische Chemie III  
Technische Universität Dortmund  
Otto-Hahn-Str. 6, 44221 Dortmund (Germany)  
Fax: (+49) 231-755-3748  
E-mail: dietmar.paschek@uni-dortmund.de

[c] Prof. Dr. R. Ludwig  
Leibniz-Institut für Katalyse, an der Universität Rostock  
Albert-Einstein-Str. 29a, 18059 Rostock (Germany)

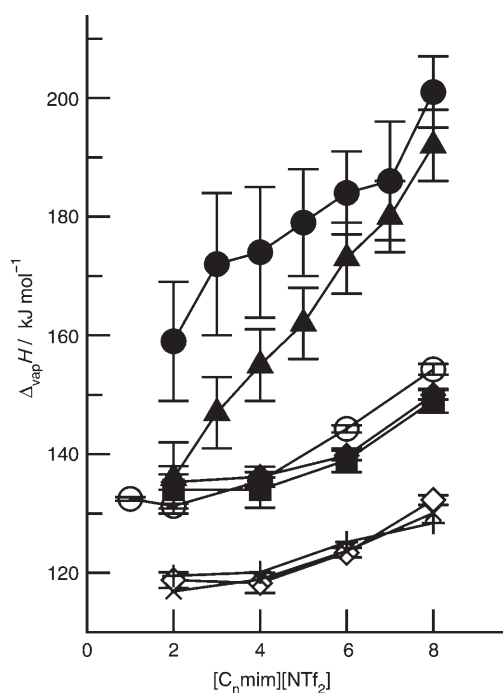


**Figure 1.** Molar enthalpies of vaporization  $\Delta_{\text{vap}}H(298)$  of  $[\text{C}_n\text{MIM}][\text{NTf}_2]$  versus alkyl chain length from the Knudsen effusion method by Zaitsau et al. ( $\blacklozenge$ ),<sup>[6]</sup> the TPD method by Armstrong et al. ( $\blacksquare$ ),<sup>[7]</sup> microcalorimetric measurements by Santos et al. ( $\blacktriangle$ ),<sup>[9]</sup> MD simulations by Santos et al. ( $\bullet$ ),<sup>[9]</sup> and our MD simulations ( $\circ$ ). Additionally  $\Delta_{\text{vap}}H(T)$  values for higher temperatures (between 463–478 K) are given from the Knudsen effusion method by Zaitsau et al. ( $\diamond$ )<sup>[6]</sup> and from COSMO-RS theory by Diedenhofen et al. (+, derived;  $\times$  directly)<sup>[13]</sup>

tions. Based on a new force field recently developed for this class of ILs we investigate heats of vaporisation as a function of temperature and alkyl chain length. In particular we want to study to which extent this property is determined by Coulomb and van der Waals interactions and thus find out what the origin of the heats of vaporisation is.

## 2. Results and Discussion

In principle, MD simulations are an appropriate method to answer these questions. Until recently, MD simulations of ionic liquids suffered from the fact that the given force fields were not able to mimic measured physicochemical properties such as the heats of vaporization, diffusion coefficients and viscosities.<sup>[10]</sup> In some cases the measured and simulated properties, such as diffusion coefficients, differed by an order of magnitude. Recently we could parameterize a refined force field for imidazolium-based ionic liquids which is capable to reproduce thermodynamic and transport properties as well as rotational correlation times from NMR measurements.<sup>[10]</sup> It is based on a former force field given by Lopez et al.<sup>[14–18]</sup> The Lennard–Jones parameters are changed in such a way that densities and diffusion coefficients for both cations and anions are brought into agreement with accurately known experimental data. It is the merit of MD simulation that the physicochemical properties can be explained on a molecular basis and by interaction ener-

gies. Herein, we apply this method to the imidazolium-based ILs  $[\text{C}_n\text{mim}][\text{NTf}_2]$  with  $n = 1, 2, 4, 6, 8$  to determine thermodynamic properties.

The heats of vaporization  $\Delta_{\text{vap}}H(T) = \Delta_{\text{l}}^{\text{g}}H_{\text{m}}^{\text{g}}(T)$  were calculated from the differences between the molar internal energies of the gas and the liquid phases  $\Delta_{\text{l}}^{\text{g}}U_{\text{c,m}}(T)$  and  $RT$  [Eq. (1)].

$$\Delta_{\text{vap}}H(T) = \Delta_{\text{l}}^{\text{g}}H_{\text{m}}^{\text{g}}(T) = \Delta_{\text{l}}^{\text{g}}U_{\text{c,m}}(T) + RT \quad (1)$$

where  $R$  represents the gas constant. The gas phase was assumed to consist purely of isolated ion pairs. This assumption is in agreement with experimental findings by Armstrong et al.,<sup>[7]</sup> Emel'yanenko et al.,<sup>[8]</sup> and Leal et al.,<sup>[19]</sup> as well as with MD simulations of the neat liquid,<sup>[10]</sup> clusters<sup>[11]</sup> and nanometric droplets<sup>[12]</sup> of ionic liquids. For calculating  $\Delta_{\text{l}}^{\text{g}}U_{\text{c,m}}(T)$ , inter- and intramolecular contributions were considered separately. The intramolecular contributions contained bonded interactions, such as bonds, bond-bending, dihedral interactions, as well as non-bonded intramolecular contributions, including specifically scaled 1–4 interactions. No cutoffs were applied for intramolecular interactions [Eq. (2)].

$$\Delta_{\text{l}}^{\text{g}}U_{\text{c,m}} = [U_{\text{gas}}(\text{inter}) - U_{\text{liquid}}(\text{inter})] + [U_{\text{gas}}(\text{intra}) - U_{\text{liquid}}(\text{intra})] \quad (2)$$

In addition, the intermolecular interactions were further divided into electrostatic and Lennard–Jones components, to make a clear distinction between Coulomb and van der Waals contributions to the total cohesive energies. For the isolated ion pair in the gas phase, interactions between all site–site pairs were explicitly considered and no distance cutoffs applied. For the condensed phase, the electrostatic energy was computed by applying the Ewald summation with tinfoil boundary conditions. To ensure that only intermolecular contributions were included, the molecular Ewald self-correction term was applied to all intramolecular interaction pairs. The reciprocal lattice term was calculated by using a smooth particle mesh Ewald method.<sup>[20]</sup> For the Lennard–Jones interactions isotropic cutoff corrections were applied. Cutoff distances (1.5 nm), Ewald convergence parameters ( $3.4 \cdot 10^{-5} \text{ nm}^{-1}$ ) and reciprocal lattice dimensions (42 grid points per dimension with interpolation order 4) were chosen to provide practically converged data. Since GROMACS<sup>[21,22]</sup> does not routinely allow a clean separation between inter- and intramolecular contributions, the energy analysis was performed a posteriori by employing the *trajenergy* program, which is part of the MOSCITO MD simulation suite of programs (available upon request).<sup>[23]</sup> The a posteriori computed total potential energies reproduce the total energies originally provided by GROMACS. The simulated values for  $\Delta_{\text{vap}}H(298)$  are shown in Figure 1. We obtain values of about  $132.5 \text{ kJ mol}^{-1}$  for  $[\text{C}_1\text{mim}][\text{NTf}_2]$ ,  $130.6 \text{ kJ mol}^{-1}$  for  $[\text{C}_2\text{mim}][\text{NTf}_2]$ ,  $135.1 \text{ kJ mol}^{-1}$  for  $[\text{C}_4\text{mim}][\text{NTf}_2]$ ,  $143.8 \text{ kJ mol}^{-1}$  for  $[\text{C}_6\text{mim}][\text{NTf}_2]$ , and  $153.6 \text{ kJ mol}^{-1}$  for  $[\text{C}_8\text{mim}][\text{NTf}_2]$ . The heats of vaporisation obtained and their increase with the alkyl chain length are in very good agreement with experimental values from the Knudsen-effusion method<sup>[6]</sup> as well as surface tension,<sup>[6]</sup> mass spectroscopy<sup>[7]</sup> and combus-

tion measurements.<sup>[8]</sup> Obviously the refined force field is capable of describing the internal energy of the liquid and the interaction of ion pairs correctly. The good agreement with measured heats of vaporization and their slight increase with increasing chain length of the cations allows some careful evaluation of  $\Delta_{\text{vap}}H(298)$  values obtained from other experimental methods such as microcalorimetry.<sup>[9]</sup> For the ILs  $[\text{C}_n\text{mim}][\text{NTf}_2]$  these heats of vaporization (Figure 1) are significantly higher than those obtained from four completely different experimental methods. The MD simulations by Santos et al.<sup>[9]</sup> give even higher heats of vaporization (Figure 1). The heats of vaporization for  $[\text{C}_8\text{mim}][\text{NTf}_2]$  obtained from the Knudsen,<sup>[6]</sup> mass spectrometry<sup>[7]</sup> and surface tension measurements<sup>[6]</sup> are about  $150 \text{ kJ mol}^{-1}$ . In comparison, our MD simulations yield  $154.3 \text{ kJ mol}^{-1}$ .<sup>[10]</sup> This is in contradiction to the results obtained from the microcalorimetry measurements and the MD simulations by Santos et al.<sup>[9]</sup> For  $[\text{C}_8\text{mim}][\text{NTf}_2]$  they measured and calculated heats of vaporization between 192 and 201  $\text{kJ mol}^{-1}$ , respectively. These too-large heats of vaporization and their strong increase with alkyl chain length in the MD simulations may have their origin in overestimated Lennard–Jones interactions used in previous force fields.<sup>[14–17]</sup> If the Lennard–Jones parameters are significantly reduced to reproduce experimental diffusion coefficients—as done in the refined force field—the absolute values as well as their increase with the chain length of the imidazolium cation are described correctly. Following the procedure of Santos et al.,<sup>[9]</sup> we give a detailed analysis of the van der Waals (Lennard–Jones) and Coulomb interactions contributing to the heats of vaporization.

The merit of MD simulations is that we can now analyse the different energetic contributions which give the overall heat of vaporization. For the liquid as well as for the gas phase the following contributions can be given: the Lennard–Jones, Coulomb, kinetic and intramolecular energies (Figure 2a). The differences due to kinetic and intramolecular interactions are negligibly small and are not further considered (Figure 2a, Table 2). Typical differences in kinetic and intramolecular energies for  $[\text{C}_2\text{mim}][\text{NTf}_2]$  at 303 K are  $0.36 \text{ kJ mol}^{-1}$  and  $5.04 \text{ kJ mol}^{-1}$ , respectively. Overall it can be seen to which extent the thermodynamic properties are determined by Coulomb or van der Waals interactions and how these cohesive energies change with the alkyl chain length and temperature. This detailed study of the cohesive energy also allows interesting comparison with other normal organic solvents such as n-alcohols and n-alkanes. These relations show that the vapor pressure and heats of vaporization of ILs may serve as a reliable definition for which liquids may be regarded as ionic liquids.

The heats of vaporisation  $\Delta_{\text{vap}}H(T)$  are mainly given by the differences between the molar internal energy of the liquid and the gas phases,  $\Delta_{\text{vap}}U$  [Eq. (1)]. The internal energy for each phase can be divided into the Coulomb and van der Waals interactions as well as minor con-

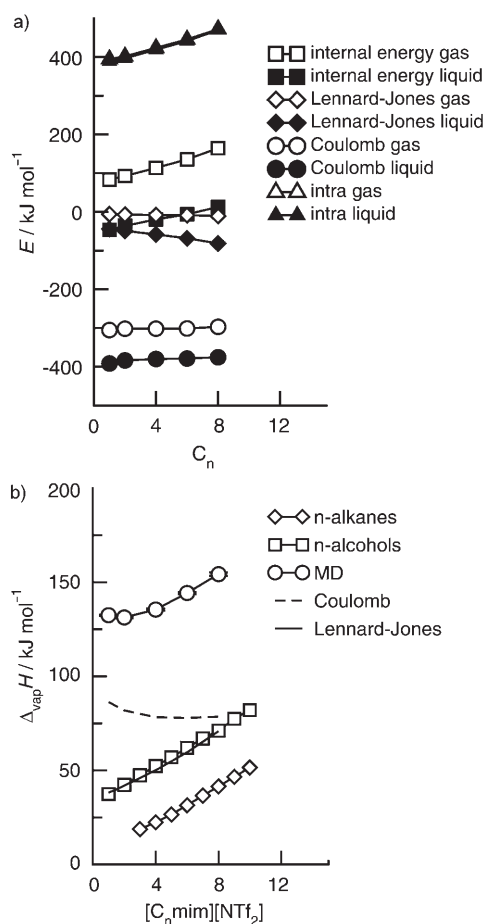


**Figure 2.** a) Energetic contributions for the gas (open symbols) and the liquid phase (filled symbols) of  $[\text{C}_n\text{MIM}][\text{NTf}_2]$  from our MD simulations. The differences of the Coulomb and van der Waals contributions of both phases mainly contribute to the overall heats of vaporisation as shown in Figure 2b. The symbols ( $\Delta$ ) for the “intra-gas” and “intra-liquid” contributions are superimposed. b) Molar enthalpies of vaporization  $\Delta_{\text{vap}}H(298)$  for  $[\text{C}_n\text{MIM}][\text{NTf}_2]$  from our MD simulations ( $\circ$ ), from measurements of n-alkanes ( $\diamond$ ) and n-alcohols ( $\square$ ).<sup>[25–27]</sup> The Coulomb (---) and van der Waals (—) interactions from MD simulations.

tributions by intramolecular modes. The differences for the Coulomb and the van der Waals contributions are shown in Figure 2b for the ILs  $[\text{C}_n\text{mim}][\text{NTf}_2]$ . As given by Equation (1)  $\Delta_{\text{vap}}H$  and  $\Delta_{\text{vap}}U$  only differ by a constant value  $RT$  ( $=2.5 \text{ kJ mol}^{-1}$  at 298 K). Starting with  $[\text{C}_1\text{mim}][\text{NTf}_2]$  the heat of vaporisation slightly decreases to  $[\text{C}_2\text{mim}][\text{NTf}_2]$  but then constantly increases with the length of the alkyl chain of the

**Table 2.** MD-simulated enthalpies of vaporization,  $\Delta_{\text{vap}}H(298)$ , internal energies  $\Delta_{\text{vap}}U(298)$  as well as the differences between the liquid and gas phase values for the Coulomb, Lennard–Jones (van der Waals interactions), intramolecular and kinetic energies of ionic liquids  $[\text{C}_n\text{MIM}][\text{NTf}_2]$ . All properties are given in  $\text{kJ mol}^{-1}$ .

Ionic Liquid	$\Delta_{\text{vap}}H(298)$	$\Delta_{\text{vap}}U(298)$	Coulomb	Van der Waals	Intramolecular	Kinetic
$[\text{C}_1\text{MIM}][\text{NTf}_2]$	$132.1 \pm 0.3$	$129.6 \pm 0.3$	86.32	38.18	5.49	0.35
$[\text{C}_2\text{MIM}][\text{NTf}_2]$	$130.6 \pm 0.4$	$128.1 \pm 0.4$	81.86	41.86	5.04	0.36
$[\text{C}_4\text{MIM}][\text{NTf}_2]$	$135.1 \pm 0.6$	$132.6 \pm 0.6$	78.27	50.08	4.61	0.37
$[\text{C}_6\text{MIM}][\text{NTf}_2]$	$143.8 \pm 0.6$	$141.3 \pm 0.6$	77.86	59.65	4.32	0.39
$[\text{C}_8\text{MIM}][\text{NTf}_2]$	$153.6 \pm 0.9$	$151.1 \pm 0.9$	78.57	70.87	2.37	0.41

imidazolium cation. This behavior is described well by the corresponding Coulomb and van der Waals interactions. The Coulomb energy is constant for all ILs and not influenced by the increasing chain length.  $[C_1\text{mim}][\text{NTf}_2]$  shows a slightly higher Coulomb contribution as reflected in the heats of vaporisation. This effect can be attributed to the symmetry of the cation. Methyl groups at both positions, C(1) and C(3), support the Coulomb interaction. A similar effect was found by Holbrey et al.<sup>[24]</sup> for the melting points ( $T_m$ ) of 1-alkyl-3-imidazolium/ $\text{NTf}_2$ . Going from  $[C_1\text{mim}][\text{NTf}_2]$  to  $[C_2\text{mim}][\text{NTf}_2]$   $T_m$  decreases by more than 20 K. It is exactly this Coulomb contribution which is responsible for the slightly larger heat of vaporisation for  $[C_1\text{mim}][\text{NTf}_2]$  over  $[C_2\text{mim}][\text{NTf}_2]$ . Overall the Coulomb energy is smaller than expected for a system completely composed of ions. As seen in Figure 2b the increase of the heats of vaporisation  $\Delta H_{\text{vap}}$  along the homologous series is completely dominated by van der Waals interactions. They show the same increase with alkyl chain length as the heats of vaporisation. Similar behavior was found by Santos et al.<sup>[9]</sup>

They referred their measured increase in the heat of vaporisation of about  $8.9 \pm 0.1 \text{ kJ mol}^{-1}$  for each  $\text{CH}_2$  group to the trend observed for the heat of condensation  $\Delta_{\text{con}}H$  for the solid-phase  $n$ -alkane family.<sup>[25–27]</sup> In our view a comparison of properties for different systems (ILs,  $n$ -alcohols,  $n$ -alkanes) describing the same phase transition (here liquid/gas) is perhaps more appropriate. Thus we show the heats of vaporisation  $\Delta_{\text{vap}}H(298)$  of the  $n$ -alkanes and  $n$ -alcohols in Figure 2b for comparison. It is seen that the van der Waals interactions of the ILs  $[C_n\text{mim}][\text{NTf}_2]$  show exactly the same increase with alkyl chain length as the  $n$ -alkanes and  $n$ -alcohols. Thus the increase in heats of vaporisation for imidazolium-based ILs arises completely from van der Waals interactions. For each  $\text{CH}_2$  group  $4.95 \text{ kJ mol}^{-1}$  is reported for  $n$ -alkanes and  $n$ -alcohols.<sup>[26]</sup> In our MD simulations the van der Waals interactions of the ILs increase by  $4.7 \text{ kJ mol}^{-1}$  per methylene group ( $n=1-8$ ). Benson<sup>[28]</sup> could show that the difference in heats of vaporisation of  $n$ -alcohols and their analogous hydrocarbons is  $25.5 \text{ kJ mol}^{-1}$  at 298 K. He concluded that this difference represents the contribution of the hydrogen bond to the value of  $\Delta_{\text{vap}}H(298)$  for  $n$ -alcohols. In this sense we can conclude that the Lennard–Jones contributions in the MD simulations comprise the pure van der Waals interaction and the hydrogen bond energy. The difference to the  $\Delta_{\text{vap}}H(298)$  of the ILs is represented by the Coulomb interaction only.

To illustrate the origin of the Coulomb part of the cohesive energy in both the liquid and the gas phases, we calculated coarse-grained approximate Coulomb “lattice” energies, where the ions are represented by their total charge of  $+1/-1 |e|$  lo-

cated at a certain ion-fixed position. This might be considered as the energy contribution associated with the first component of a multipole expansion of the electrostatic potential of each of the ions. The lattice energies of the condensed phase reported here were calculated using the Ewald-summation technique.

The calculated energies for  $[C_2\text{mim}][\text{NTf}_2]$  as a function of temperature (the positions of the ions are represented by their centers of mass) are shown in Figure 3a, whereas Figure 3b

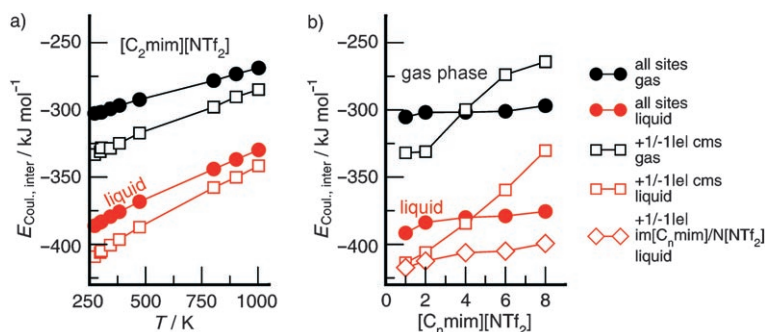


**Figure 3.** Intermolecular electrostatic interactions for  $[C_2\text{mim}][\text{NTf}_2]$ . a) As a function of temperature. b) For  $[C_n\text{mim}][\text{NTf}_2]$  as a function of alkane chain length  $n$ . Full symbols indicate energies considering all partial charges on all atoms of the ions. Open symbols represent approximate “lattice energies”, where charges of  $+1/-1 |e|$  were placed at anion and cation positions, respectively. Lattice energies for the charges being located at the ions’ centers of mass indicated by ( $\square$ ). For ( $\diamond$ ) positive charge was placed at the center of the imidazolium ring, whereas the negative charge was located on the position of the nitrogen atom of the  $[\text{NTf}_2]$  anion.

depicts energies for  $[C_n\text{mim}][\text{NTf}_2]$  as a function of alkane chain length. For short chains ( $C_1$ ,  $C_2$ ) these approximated “lattice” energies systematically overestimate the interaction energies by only about 6% and 10% in the liquid and gas phases at 273 K, respectively. The differences at higher temperatures tend to be even smaller at 3% and 6% at 1003 K. The corresponding lattice-approximated Coulomb contribution to the heat of vaporization for  $[C_2\text{mim}][\text{NTf}_2]$  underestimate the true values (considering all partial charges) over the entire temperature range by just about 6% to 10% (between 4–8  $\text{kJ mol}^{-1}$ ). This seems to be small compared to the differences in heat of vaporization reported experimentally. Taking the position of the first peak of the cation–anion center of mass pair correlation function (shown in Figure 4b) as a reference distance, we determined corresponding average Madelung constants for the  $[C_n\text{mim}][\text{NTf}_2]$  liquid. Quite remarkably, the obtained Madelung constant changes only slightly with temperature, being represented by  $1.519 \pm 0.006$  over the temperature range between 273 K and 473 K. For higher temperatures, the value decreases continuously to about 1.40 at 1003 K. The observed temperature insensitivity of the Madelung constant strongly indicates conservation of the structure of the ionic lattice over the temperature interval 273 K–473 K. The ionic lattice structure of the  $[C_n\text{mim}][\text{NTf}_2]$  liquids with anion–cation coordination numbers of about seven has great qualitative similarity with the lattice structure of 1,3-dimethylimidazolium chloride obtained from neutron diffraction.<sup>[29]</sup> Given that the ionic lattice structure of the  $[C_n\text{mim}][\text{NTf}_2]$  liquids is described correctly by our models, and the gas phase consists of isolated ion

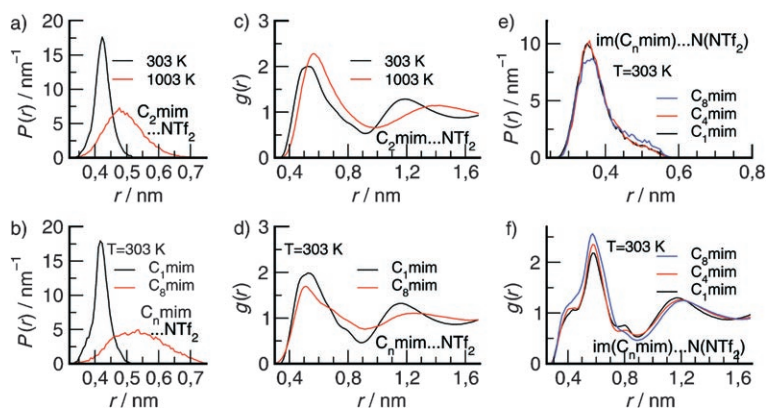


**Figure 4.** a, b) Distance distribution  $P(r)$  between the centers of mass of anion and cation for an ion pair in the gas phase for a)  $[C_n\text{mim}][\text{NTf}_2]$  at different temperatures and b) increasing alkane chain length at  $T=298\text{ K}$ . c, d) Anion–cation center of mass radial pair distribution functions  $g(r)$  for c)  $[C_n\text{mim}][\text{NTf}_2]$  at different temperatures and d) increasing alkane chain length at  $T=298\text{ K}$ . e, f) Separation between the geometric center of imidazolium group of the  $[C_n\text{mim}]$  cations and the position of the nitrogen atom in  $[\text{NTf}_2]$  for different alkane chain length at  $T=298\text{ K}$ . e) Distance–distribution obtained for an ion pair in the gas phase. f) Radial pair distribution functions in the liquid phase.

pairs, the Coulomb contribution to the heat of vaporization might be placed safely around  $70\text{--}80\text{ kJ mol}^{-1}$ . However, the situation is quite different when alkane chains of different lengths are considered. For long chain lengths, the approximated lattice energies are found to *underestimate* the cohesive energies systematically, showing a strongly increasing lattice energy, whereas the Coulomb part of the true cohesive energy varies only little with chain length. This feature was also recently reported by Santos et al.<sup>[9]</sup> and it was concluded that it provides evidence for a segregation in polar and nonpolar domains.<sup>[18]</sup> Our simulations clearly support this point of view.

When we locate the position of the  $+1/-1|e|$  charges exactly between the imidazolium ring of  $[C_n\text{mim}]$  and the position of nitrogen in  $[\text{NTf}_2]$  and calculate the corresponding lattice energies, the chain-length dependence of the true cohesive energy is recovered (see Figure 3b). The corresponding anion–cation center–center pair correlation functions even indicate an increase of the first peak with increasing chain length (Figure 4f), contrasting the behavior of the anion/cation center of mass pair correlation function given in Figure 4d. In addition, Figure 4e indicates that similar tendency to form polar contacts is also observed for the gas phase.

The contributions of Coulomb and van der Waals interactions to the heats of vaporisation  $\Delta_{\text{vap}}H(T)$  can be also studied as a function of temperature. The overall decrease of  $\Delta_{\text{vap}}H(T)$  for  $[C_2\text{mim}][\text{NTf}_2]$  from  $131.98\text{ kJ mol}^{-1}$  to  $111.30\text{ kJ mol}^{-1}$  over the temperature range of  $273\text{--}473\text{ K}$  is nearly linear (Figure 5). This decrease with temperature can be attributed to decreasing Coulomb and van der Waals interactions in a 40:60 ratio. In general it can be assumed that both the Coulomb and the van der Waals interactions will get weaker to the same extent upon decreasing densities. That the van der Waals interactions show a stronger temperature dependence could be ascribed to increasing ion pair formation.<sup>[30]</sup> The polar regions which include the imidazolium ring of the cation and the anion are

only slightly influenced by temperature, whereas the nonpolar region represented by the alkyl side chains show a stronger temperature dependence. Ion pairs keep the Coulomb interactions strong, whereas the van der Waals interactions of these neutral cluster species show significant temperature dependence. If that assumption is reliable, the analogous temperature behavior of  $\Delta_{\text{vap}}H(T)$  should be found for n-alcohols. And indeed, the decrease of  $\Delta_{\text{vap}}H(T)$  for methanol, ethanol, n-butanol, n-hexanol and n-octanol show the same negative slope as the van der Waals interactions of the imidazolium-based ionic liquids (Figure 6). This is another strong proof for the importance of van der Waals interactions in ILs as well as their increase with the alkyl chain length and decrease with increasing temperature similar to the analysis for n-alkanes and n-alcohols, respectively.

The distribution of the internal energy to Coulomb and van der Waals interactions as well as the behavior of the cohesive energies with increasing alkyl chain length and temperature have some important

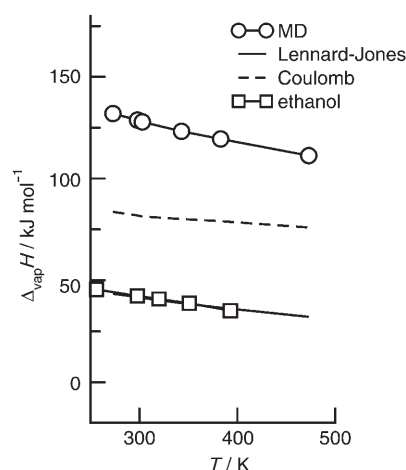


**Figure 5.** Molar enthalpies of vaporization  $\Delta_{\text{vap}}H(T)$  (○) and the contributing Coulomb (---) and van der Waals (—) interactions as a function of temperature for  $[C_2\text{MIM}][\text{NTf}_2]$  from MD simulations. For comparison the temperature-dependent  $\Delta_{\text{vap}}H(T)$  values for ethanol (□) are shown.<sup>[25–27]</sup>

implications. Based on a reliable force field, MD simulations can be used as a tool for predicting thermodynamic properties. The substantial amount of van der Waals interactions contributing the heats of vaporisation questions the use of DFT methods for describing properties of ionic liquids. As pointed out by Ballone et al.<sup>[12]</sup> and Koßmann et al.<sup>[31]</sup> most of the standard density functional approximations lack dispersion energy terms and may give cluster geometries which might be different from the true ones.

Recent articles stated that many-body effects have to be included into the force fields to ensure accurate predictions of the structure and dynamics of ionic liquids.<sup>[32–34]</sup> In particular, transport properties such as self-diffusion and viscosity would deviate significantly from experimental data if only simple pair-

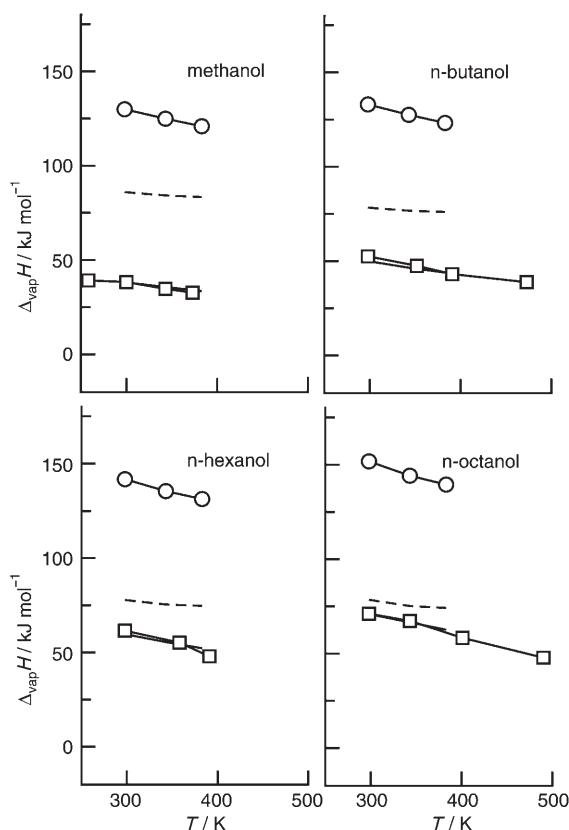


**Figure 6.** Molar enthalpies of vaporization  $\Delta_{\text{vap}}H(T)$  (○) and the contributing Coulomb (---) and van der Waals (—) interactions as a function of temperature for  $[\text{C}_n\text{MIM}][\text{NTf}_2]$  with  $n = 1, 4, 6,$  and  $8$  from MD simulations. For comparison the temperature-dependent  $\Delta_{\text{vap}}H(T)$  values for the analogous  $n$ -alcohols (□) are given.<sup>[25–27]</sup> a) methanol, b)  $n$ -butanol, c)  $n$ -hexanol and d)  $n$ -octanol. The corresponding data for  $n = 2$  ( $[\text{C}_2\text{MIM}][\text{NTf}_2]$ ) and ethanol are already shown in Figure 5.

wise-additive force fields are used. Our study suggests that averaged polarization effects were also described reasonably by an effective two-body force field. For the heats of vaporization it could be argued the contributions in the gas and the liquid phase cancel out each other. Previously, we could show that transport properties could be simulated with reasonable accuracy and that they reflect the dependency with temperature and alkyl chain length.<sup>[10]</sup>

### 3. Conclusions

Using a refined force field for describing ILs  $[\text{C}_n\text{mim}][\text{NTf}_2]$  with  $n = 1, 2, 4, 6, 8$  we studied the heats of vaporisation and their behavior with changing alkyl chain length and temperature. The different parts of the cohesive energies contributing to the overall heats of vaporisation were discussed in detail. Whereas the Coulomb contributions remain almost constant around  $80 \text{ kJ mol}^{-1}$  with increasing alkyl chain length, the contribution attributed to the van der Waals interactions is found to increase continuously. Approximate “lattice” energies are found to be the dominant contribution to the electrostatic cohesive energy. In line with previous observations, a polar/nonpolar segregation (ion pair formation) is observed for longer chain

lengths and is responsible for Coulomb energies which are almost independent of the alkane chain length. The calculated increase of the heat of vaporisation of about  $4.7 \text{ kJ mol}^{-1}$  per  $\text{CH}_2$ -group exactly matches the increase of the heats of vaporisation of  $n$ -alcohols and  $n$ -alkanes. Additionally, the temperature dependence of the van der Waals energies of the imidazolium-based ionic liquids is also found to match to the temperature behavior of the  $\Delta_{\text{vap}}H$  data of alcohols. Our simulations highlight the importance of the van der Waals interactions even for a system consisting purely of ions. The MD results also suggest that Knudsen effusion<sup>[6]</sup> and mass spectrometry<sup>[7]</sup> are the most suitable methods for determining heats of vaporization.

### Computational Methods

Classical molecular dynamics simulations of liquid  $[\text{C}_n\text{mim}][\text{NTf}_2]$  with  $n = 1, 2, 4, 6, 8$  were carried out in the isobaric–isothermal (NPT) ensemble by using a new force field described recently.<sup>[10]</sup> The simulated systems consist of 173 ion pairs at 1 bar. The simulations were carried out using the Gromacs–MD package<sup>[21,22]</sup> at temperatures of 273, 303, 343, 383, 473, 803, 903 and 1003 K. For the liquid-phase simulations electrostatic interactions were computed by using the smooth particle mesh Ewald-summation method<sup>[20]</sup> with fourth-order interpolation and 0.12 mesh spacing, a Ewald convergence factor of  $3.4 \text{ nm}^{-1}$ , and by applying a cut-off radius of 1.2 nm. Appropriate isotropic Lennard–Jones long-range corrections for pressure and energy were considered. For simulations of the ion pair in the gas phase no periodic boundary conditions and cutoffs were used, and the initial linear and angular momenta were removed. Temperature and pressure control was achieved using a Nosé–Hoover thermostat<sup>[35,36]</sup> and the Rahmann–Parrinello barostat.<sup>[37,38]</sup> with coupling times of  $\tau_T = 0.5 \text{ ps}$  and  $\tau_P = 2 \text{ ps}$ . Each of the simulation runs of the condensed phases was 10 ns long. Integration time steps of 2 fs were used. All bond lengths involving hydrogen atoms were held fixed by using the SHAKE algorithm.<sup>[39]</sup> The heats of vaporisation ( $\Delta_{\text{vap}}H$ ) were calculated from the differences of the internal energies between the liquid and the gas phases for the ionic liquids at the given temperatures. The further energy analysis was computed a posteriori from stored trajectory data. Details are given in the Results and Discussion section.

### Acknowledgements

Financial support by the state of Mecklenburg–Vorpommern, Germany, is gratefully acknowledged.

**Keywords:** cohesion energy · enthalpies of vaporization · ionic liquids · molecular dynamics · thermodynamics

- [1] *Ionic Liquids in Synthesis* (Ed.: P. Wasserscheid and T. Welton), 2nd Edition, Wiley-VCH, Weinheim, 2007.
- [2] R. D. Rogers and K. R. Seddon, *Science* **2003**, 302, 792–793.
- [3] F. Endres and S. Zein El Abedin, *Phys. Chem. Chem. Phys.* **2006**, 8, 2101–2116.
- [4] M. J. Earle, J. M. S. S. Esperança, M. A. Gilea, J. N. Canongia Lopes, L. P. N. Rebelo, J. W. Magee, K. R. Seddon and J. A. Widegren, *Nature* **2006**, 439, 831–834.
- [5] P. Wasserscheid, *Nature* **2006**, 439, 797.
- [6] D. H. Zaitsau, G. J. Kabo, A. A. Strechan, Y. U. Paulechka, A. Tschersich, S. P. Verevkin and A. Heintz, *J. Phys. Chem. A* **2006**, 110, 7303–7306.

- [7] J. P. Armstrong, C. Hurst, R. G. Jones, P. Licence, K. R. J. Lovelock, C. J. Satterley and I. J. Villar-García, *Phys. Chem. Chem. Phys.* **2007**, *9*, 982–990.
- [8] V. N. Emel'yanenko, S. P. Verevkin and A. Heintz, *J. Am. Chem. Soc.* **2007**, *129*, 3930–3937.
- [9] L. M. N. B. F. Santos, J. N. C. Lopes, J. A. P. Coutinho, J. M. S. S. Esperança, L. R. Gomes, I. M. Marrucho and L. P. N. Rebelo, *J. Am. Chem. Soc.* **2007**, *129*, 284–285.
- [10] T. Köddermann, D. Paschek, R. Ludwig, *ChemPhysChem* **2007**, *8*, 2464–2470.
- [11] M. S. Kelkar, E. J. Maginn, *J. Phys. Chem. B* **2007**, *111*, 9424–9427.
- [12] P. Ballone, C. Pinilla, J. J. Kohanoff, M. G. Del Pópolo, *J. Phys. Chem. B* **2007**, *111*, 4938–4950.
- [13] M. Diederhofen, A. Klamt, K. Marsh, A. Schäfer, *Phys. Chem. Chem. Phys.* **2007**, *9*, 4653–4656.
- [14] J. N. Canongia Lopes, J. Dechamps, A. A. H. Pádua, *J. Phys. Chem. B* **2004**, *108*, 2038–2047.
- [15] J. N. Canongia Lopes, A. A. H. Pádua, *J. Phys. Chem. B* **2004**, *108*, 16893–16898.
- [16] J. N. Canongia Lopes, A. A. H. Pádua, *J. Phys. Chem. B* **2006**, *110*, 7485–7489.
- [17] J. N. Canongia Lopes, M. F. C. Gomes, A. A. H. Pádua, *J. Phys. Chem. B* **2006**, *110*, 16816–16818.
- [18] J. N. Canongia Lopes, A. A. H. Pádua, *J. Phys. Chem. B* **2006**, *110*, 3330–3335.
- [19] J. P. Leal, J. M. S. S. Esperança, M. E. Minas da Piedade, J. N. Canongia Lopes, L. P. N. Rebelo, K. R. Seddon, *J. Phys. Chem. A* **2007**, *111*, 6176–6182.
- [20] U. Essmann, L. Perera, M. L. Berkowitz, T. A. Darden, H. Lee, L. G. Pedersen, *J. Chem. Phys.* **1995**, *103*, 8577–8593.
- [21] E. Lindahl, B. Hess, D. van der Spoel, *J. Mol. Model.* **2001**, *7*, 306–317.
- [22] D. van der Spoel, A. R. van Buuren, E. Apol, *Gromacs User Manual Version 3.1*, AG Groningen, The Netherlands, **2001**. <http://www.gromacs.org>.
- [23] D. Paschek, *MOSCITO–4-MD Simulation Package*, **2007** (<http://ganter-chemie.uni-dortmund.de/MOSCITO>).
- [24] J. D. Holbrey, W. M. Reichert, R. D. Rogers, *Dalton Trans.* **2004**, 2267–2271.
- [25] J. S. Chickos, W. E. Acree, Jr., *J. Chem. Eng. Data* **2003**, *32*, 1800–2007.
- [26] J. S. Chickos, W. Hanshaw, *J. Chem. Eng. Data* **2004**, *49*, 620–630.
- [27] D. Matulis, *Biophys. Chem.* **2001**, *93*, 67–82.
- [28] S. W. Benson, *J. Am. Chem. Soc.* **1996**, *118*, 10645–10649.
- [29] C. Hardacre, J. D. Holbrey, S. E. J. McMatch, D. T. Bowron, A. Soper, *J. Chem. Phys.* **2003**, *118*, 273–278.
- [30] T. Köddermann, C. Wertz, A. Heintz, R. Ludwig, *ChemPhysChem* **2006**, *7*, 1944–1949.
- [31] S. Kossmann, J. Thar, B. Kirchner, P. A. Hunt, T. Welton, *J. Chem. Phys.* **2006**, *124*, 174506.
- [32] O. Borodin, G. D. Smith, *J. Phys. Chem. B* **2006**, *110*, 6293–6299.
- [33] O. Borodin, G. D. Smith, *J. Phys. Chem. B* **2006**, *110*, 11481–11490.
- [34] O. Borodin, G. D. Smith, W. Henderson, *J. Phys. Chem. B* **2006**, *110*, 16879–16886.
- [35] S. Nosé, *J. Chem. Phys.* **1984**, *52*, 255–268.
- [36] W. G. Hoover, *Phys. Rev. A*, **1985**, *31*, 1695–1697.
- [37] A. Rahman, M. Parrinello, *J. Appl. Phys.* **1981**, *52*, 7182–7190.
- [38] S. Nosé, M. L. Klein, *Mol. Phys.* **1983**, *50*, 1055–1076.
- [39] J. P. Ryckaert, G. Ciccotti, H. J. C. Berendsen, *J. Comput. Phys.* **1977**, *23*, 327–341.

Received: December 6, 2007

Revised: January 3, 2008

Published online on February 18, 2008